International Journal of Applied Pharmaceutics

ISSN- 0975-7058 Vol 18, Issue 1, 2026

Original Article

INVESTIGATION ON FORMULATION VARIABLES FOR PREPARATION OF FLUCONAZOLE-LOADED SPANETHOSOMES

SAJATAHER SAHIB[1], LUBNA A. SABRI[2*]

[1]College of Pharmacy, University of Misan, Iraq. [2]Department of Pharmaceutics, College of Pharmacy, University of Baghdad, Iraq
*Corresponding author: Lubna A. Sabri; *Email: lobna.sabri@copharm.uobaghdad.edu.iq

Received: 21 Jul 2025, Revised and Accepted: 24 Oct 2025

ABSTRACT

Objective: This study aimed to develop fluconazole (FLC)-loaded spanethosomes by investigating the effects of various formulation variables, with the goal of identifying the optimal formulation that exhibits desirable vesicular characteristics for topical delivery.

Methods: Fifteen formulations containing 0.5% w/v FLC spanethosomes were prepared using the ethanol injection method. The formulations were assessed for vesicle size, polydispersity index (PDI), entrapment efficiency and in vitro drug release. The optimal formulation was further characterized for its morphological features and FTIR spectra.

Results: All prepared spanethosomes exhibited nanoscale vesicle sizes ranging between 79±8.54 and 3517±80.85 nm, with entrapment efficiency between 42.35±4.55 and 95.46±0.68%. The optimum formula, composed of Span 60 and sodium deoxycholate (SDC) in a 200:15 mg weight ratio, exhibited a spherical morphology without aggregation. It achieved a cumulative FLC release of 94.6% within 6 h.

Conclusion: These results suggest that spanethosomes are promising drug delivery systems that can enhance the therapeutic efficacy of FLC for treating superficial fungal infections while minimizing systemic side effects.

Keywords: Ethanol injection, Formulation optimization, Fluconazole, Spanethosomes, Topical delivery

DOI: https://dx.doi.org/10.22159/ijap.2026v18i1.56187 Journal homepage: https://innovareacademics.in/journals/index.php/ijap

INTRODUCTION

Fungal infections have markedly increased in recent years and are now acknowledged as a significant new concern to millions worldwide. The most common fungal diseases are superficial infections of the skin and nails, primarily caused by dermatophytes [1].

Options for treatment of fungalinfections may be classified as systemic or topical. Traditional systemic therapies are frequently avoided due to several risks, including organ injury, drug deposits, interactions with other drugs, and elevated medical expenses [2]. Today, topical and transdermal therapies provide simplicity of application and enhanced patient adherence, rendering them more advantageous [3].

Fluconazole (FLC) belongs to the third generation triazole-based multi-functional antifungal agent. It has a broadspectrum activity that can be utilized for the prevention and treatment of superficial and systemic fungal infections. Fluconazole is slightly soluble in water (5 mg/ml at 37 °C) and has moderate lipophilicity (logP equal 0.5). Although both oral and parenteral injections are commercially available to deliver FLC, they may result in GIT upset, floating, hematological changes, rashes and hepatotoxicity [4]. Subsequently, FLC topical formulation is represented an alternative approach to reduce systemic undesired effects. A study conducted by Salerno *et al.* (2010) focused on the development of various topical formulations (including; emulsions, emulgels, lipogels, and microemulsion-based hydrogels) to enhance the therapeutic efficacy and skin penetration of FLC. The researchers demonstrated that microemulsion-based systems, particularly those containing Transcutol® as a penetration enhancer, achieved superior FLC release profiles and significantly improved percutaneous absorption through pig skin, delivering nearly the entire dose to the target site. In contrast, the conventional formulations like lipogels delivered only about half of the applied dose into the skin [5].

In recent decades, numerous topical nanovesicles as drug carriers have been created to address challenges related to drug solubility and limited penetration through stratum corneum. They facilitated sustained drug delivery by enhancing epidermal/dermal drug depositions, thereby minimizing systemic side effects [6]. Most nanovesicles are characterized by highly organized concentric bilayers that self-assemble and mature upon contact with an aqueous phase containing amphiphilic building blocks, including nonionic surfactants and phospholipids. These vesicles demonstrate significant safety, biocompatibility, and the capacity to encapsulate both hydrophilic and lipophilic chemical compounds [7].

Traditional nanovesicles such as liposomes and niosomes have difficulties in effectively delivering the medicine through the skin [8]. In response, novel deformable nanovesicle systems such as, ethosomes, transferosomes, transethosomes and spanlastics have been developed. Spanlastics, a flexible nanovesicular system, are capable of delivering diverse of the pharmacological agents, demonstrates potential as a drug delivery vehicle. Spanlastic has multiple advantages compared to conventional vesicular systems used topically, such as increased stability, adaptability in penetration, and superior targeting efficacy [9]. A novel generation of spanlastics is designated as spanethosomes, achieved by integrating ethanol into the spanlastics' structure. This synergistic combination of Span, edge activator, and ethanol is anticipated to facilitate the restructuring of the vesicular bilayer, leading to surface irregularity, improved elasticity, and greater permeability across the skin [10]. Ethanol is widely recognized as an excellent penetration enhancer, as it intercalates with the hydrophilic regions of the intercellular lipid domains of the stratum corneum, resulting in a reduction of the lipid melting point, hence increasing lipid fluidity and cell membrane permeability. Furthermore, ethanol in ultradeformable formulations renders the membrane bilayers less thick and highly pliable, resulting in the creation of more deformable and flexible vesicles capable of easily traversing the minute apertures generated in the disrupted stratum corneum lipids [11].

The aim of this study is to develop and optimize FLC-loaded spanethosomes as a novel topical delivery system to enhance the therapeutic efficacy of FLC for superficial fungal infections while minimizing systemic side effects. The study mainly focuses on investigating the impact of various formulation variables including; Span amount, edge activator type and ethanol volume on the physicochemical characteristics of the prepared vesicles.

MATERIALS AND METHODS

Materials

FLC was gifted from Sama-alfayhaa Pharmaceutical Industry; Iraq. Span 60 (sorbitanmonostearate) was purchased from alpha chemika, India. Tween 80 and ethanol were from (loba chemie pvt, Ltd, India. Sodium deoxycholate SDC was from HIMEDIA labritories, India. Phosphate buffer 5.5 (Himedia Laboratories, India). Dialysis membrane, molecular weight 8000-14000 Da (Special products laboratory, USA).

Preparation of fluconazole-loaded spanethosomes

An attempt was made to prepare SEs using the ethanol injection method [9]. Briefly, an ethanolic solution of 0.5% w/v FLC and Span 60 at varying concentrations (1, 2, and 1.5% w/v) was injected slowly into a beaker containing Tween 80 (50, 75,100, 150 mg) dissolved in deionized water. In a separate set of preparation, sodium deocxycholate (SDC) was added at amount (5, 10 and 15 mg). The mixture was continuously stirred using homogenizer (HG-150, Witeg Labortechink, Germany) at 2000 rpm for 10 min, followed by stirring with magnetic stirrer (Witeglabortechnik GmbH, Korea) at 1500 rpm for 30 min. In order to reduce particle size, the resulting dispersion was subjected to probe sonication (QSON ICA Sonicator, Qsonica, USA). The sonicator was set up with a pulse cycle of 50 seconds on and 10 seconds off, amplitude of 30%, and a total sonication time of 5 min. A 1/8-inch diameter probe was used for the process [12]. Table 1 showed the composition of fifteen prepared FLC-loaded spanethosomes dispersion. The obtained dispersion was then refrigerated overnight to allow vesicle maturation and stored under refrigeration until further physicochemical characterization.

Table 1: Formulation composition of FLC-loaded spanethosomes

Formula code	FLC (mg)	Span 60 (mg)	Ethanol (ml)	Tween 80 (mg)	SDC (mg)	Deionized water q. s to (ml)
F1	50	100	2	75	0	10
F2	50	100	3	75	0	10
F3	50	100	4	75	0	10
F4	50	200	2	75	0	10
F5	50	200	3	75	0	10
F6	50	200	4	75	0	10
F7	50	300	2	75	0	10
F8	50	300	3	75	0	10
F9	50	300	4	75	0	10
F10	50	200	3	50	0	10
F11	50	200	3	100	0	10
F12	50	200	3	150	0	10
F13	50	200	3	0	5	10
F14	50	200	3	0	10	10
F15	50	200	3	0	15	10

Charecterization of FLC-SEs formulation

Determination of FLC entrapment efficiency percent (EE %)

The indirect method has been employed to determine the EE% of FLC in the spanethosomes. Total amount of FLC added in each formulation was subtracted from the amount of unentrapped (free) FLC present in the dispersion media. To separate free FLC from spanethosomes, 1 ml of spanethosomes dispersion was placed in an eppendorf tube and rotated using colding centrifuge at 15000 rpm for 1 hour at 7 ℃. The supernatant was then collected and appropriately diluted with ethanol. The concentration of free FLC was quantified by measuring drug absorbance using a UV-VIS spectrophotometer at 261 nm. The amount of free FLC was then determined using previously establisheddrug-absorbance calibration question (y=0.0021x-0.0114, R^2=0.9993). The EE% was then calculated using the following equation [13]:

$$EE\% = \frac{\text{Total amount of FLC} - \text{amount of free FLC}}{\text{Total amount ofFLC}} \times 100$$

Particle size and PDI analyzer

The size of the spanethosome vesicles is a critical for their penetration into the skin; smaller vesicles or particles penetrate more profoundly. By employing a 5mW neon laser and a Nano ZS90 (Malvern Instrument Ltd. UK), the average vesicles size and PDI were determined. An expandable polymeric cell with a diameter of 10 mm and a runtime of 180 s was employed to conduct the analysis at ambient temperature of 25 ℃at a 170° angle [14].

In vitro drug release of the selected spanethosomes formulations

The drug release from the spanethosomes was conducted for 6 h at 100 rpm using the paddle method. The dissolving medium's temperature was maintained at 32±1 °C. The saturated solubility of fluconazole in phosphate buffer pH 5.5, as dissolution medium, was previously determined to be approximately 3.07 mg/ml. The spanethosomes dispersion corresponding to 50 mg of FLC was evaluated in the vitro release study. A volume of 150 mL of dissolution medium was employed, which is sufficient to dissolve more than nine times the total drug content. Therefore, the amount of drug released at each time point remained below saturation solubility, confirming that sink conditions were maintained throughout the experiment. At specified intervals, three milliliters of the dissolving medium were withdrawn, and an equivalent volume of fresh dissolution medium was concurrently added to the apparatus to maintain a consistent volume. The removed samples were tested spectrophotometrically at 260 nm [15].

Fourier-transform infrared spectra (FTIR) and x-ray diffraction analysis

The physical and chemical compatibility as well as crystallinity status were assessed using Fourier-transform infrared spectroscopy (FTIR) and X-ray diffractometer, respectively. These analyses included the pure FLC, a physical mixture of FLC, span 60 and SDC in a 1:1:1 ratio as well as the selected formulation. The FTIR measurement was performed using a (Shimadzu FTIR-1800 spectrometer, Japan). Samples were directly applied onto the crystal spectra data were recorded over the range of 4000–400 cm^{-1} to evaluate potential interactions and structural characteristics [16]. The X-ray diffraction analysis was performed using (Malvenpanalytical, Aeris, UK) diffractometer equipped with a copper (Cu) X-ray source. The diffraction patterns were recorded over a 2θ range spanning from 5° to 90°. Diffractograms were captured at room temperature with a voltage of 45 kV, a current of 30 mA [17].

Assessment of FLC stability in spanethosome formulations using HPLC-UV

The stability of the FLC-loaded spanethosome formulation (F15) was assessed after 3 mo of storage at room temperature to verify that no degradation or chemical changes had occurred. This was done by comparing retention times. Samples were analyzed using a high-performance liquid chromatography (HPLC) system (SYKAM,

Germany), equipped with a C18-ODS column (25 cm × 4.6 mm). The mobile phase consisted of a buffer: acetonitrile mixture (80:20) adjusted to pH 5 with acetic acid. Detection was performed at 260 nm using a UV detector, with a flow rate of 1 ml/min. The retention time of FLC in the freshly prepared F15 formulation and its blank was compared with that of the same formulation stored at room temperature for 3 mo. The consistency in retention times indicated no significant degradation or alteration in the chemical composition of the formulation during the storage period [18].

Surface morphology determination

An aliquot of the optimal spanethosomes formula dispersion was examined under an optical microscope to verify vesicle formation and their homogeneity. The surface morphology was also investigated using Field Emission Scanning Electron Microscopy. The samples were evenly distributed on double-sided carbon adhesive tapes and mounted onto SEM stubs. To enhance conductivity and improve image quality, a uniform thin layer of conductive material was applied to the samples via sputter coating for two minutes prior to imaging [19].

Statistical analysis

The results of all evaluation tests were reported as the mean±SD, and they were done in triplicate. For the statistical analysis, GraphPad Prism 10.5.0 conducted a one-way ANOVA. Statistical significance was determined by P values of 0.05 or less, while values exceeding 0.05 were considered statistically insignificant.

RESULTS AND DISCUSSION

Preparation of fluconazole-loadedspanethosomes

A uniform, milky-white liquid dispersion was the appearance of the fifteen prepared formulas. The results of the investigation the effects of the formulation variables, which include varying amounts of span60, ethanol volume, the amount of SDC and tween80, on the characteristics of spanethosome vesicles are revealed in table 2.

The nanosize of spanethosomes was varying between 79±8.54 and 3517±80.85 nm, and the PDI ranged from 0.06±0.02 to 0.51±0.01. Meanwhile, the EE % data ranged from 42.35±4.55 to 95.46±0.68%.

Table 2: The spanethosomal vesicular size, PDI and entrapment efficiency % of the prepared formulas

Formula code	Vesicles size (nm)*	PDI*	EE (%)*
F1	79.00±8.54	0.25±0.02	42.35±4.55
F2	301.00±18.52	0.06±0.02	94.34±2.18
F3	3517.00±80.85	0.35±0.01	87.63±7.81
F4	224.33±10.02	0.51±0.01	89.94±10.35
F5	186.33±13.05	0.19±0.01	91.41±8.35
F6	1803.00±25.94	0.24±0.02	94.97±1.67
F7	233.67±14.84	0.46±0.01	85.74±1.31
F8	202.00±17.52	0.28±0.02	70.86±3.63
F9	745.33±32.25	0.21±0.01	92.87±3.10
F10	277.77±11.11	0.42±0.02	45.74±1.10
F11	158.73±10.00	0.27±0.02	78.25±0.90
F12	151.33±9.02	0.21±0.02	64.47±0.72
F13	277.17±18.41	0.41±0.01	95.46±0.68
F14	185.00±5.00	0.38±0.01	90.87±0.45
F15	188.7±1.80	0.25±0.01	91.91±0.80

*The results were presented as the mean±SD, n=3.

Characterization of FLC entrapment efficiency percent

At constant span amount and tween amount, the effect of ethanol volume on the EE% of FLC-loaded spanethosomes was shown in fig. 1. There was high significant ($p<0.05$) increase in EE% with increase ethanolas in grouped F3>F2>F1 fig. 1A. Meanwhile, increasing ethanol volume showed a non-significant ($P>0.05$) difference in EE% when 200 mg of span60 used as shown in fig. 1B. At higher span 60 amount (300 mg), there was significant decrease in EE% with increase ethanol volume as shown in fig. 1C. These findings were well related with the studies done by Bhalaria M [20] and Almajidi YQ [14] who incorporated ethanol as a cosolvent, observed enhanced solubility of the active pharmaceutical ingredient, that enabling greater entrapment within both the hydroalcoholic core and the vesicular membrane. Ethanol also contributes to increased fluidity of the lipid bilayer, thereby facilitating improved encapsulation of drug. However, further increase in ethanol volume appears to disrupt membrane integrity by enhancing permeability, which may result in a decrease in the overall entrapment efficiency of the ethosomal formulations. The low EE% observed of formula F1, despite its small size (79 nm) may potentially due to surface-associated drug loss or vesicle instability.

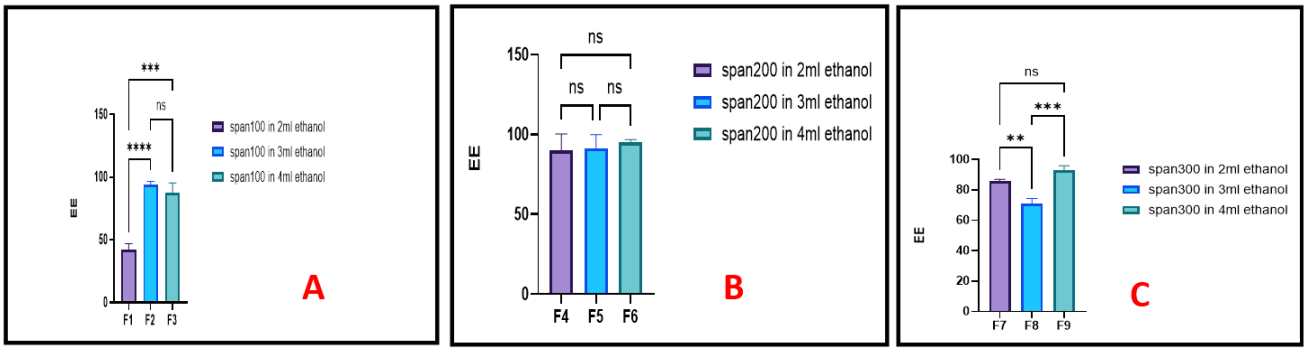

Fig. 1: The impact of ethanol volume on the entrapment efficiency of FLC-loaded spanethosomescontaining; (A) 100 mg Span 60, (B) 200 mg Span 60 and (C) 300 mg Span 60, (ns,*, ** and * represent non-significant, P<0.05, P<0.01 and P<0.001 respectively), n=3, mean values±SD**

On the other hand, an increase in Span 60 concentration from 100 mg to 200 mg and 300 mg, across various ethanol concentrations, resulted in a significant enhancement in EE%. This improvement may be attributed to a reduction in interfacial energy and an increase in the dispersion's viscosity, both of which help to minimize drug leakage from the vesicles. Moreover, Span 60 is nonionic surfactant with a long alkyl chain (C18) and low hydrophilic-lipophilic balance (HLB) value that contributes to the formation of a more rigid and stable lipid bilayer, thereby further enhancing EE% by reducing drug diffusion, even at higher ethanol concentrations [21, 22].

Notably, formulations F10–F15 were designed to directly compare the effects of Tween 80 and SDC along with their concentrations under identical conditions, while keeping all other components constant. As shown in fig. 2A, there was a statistically significant ($p<0.05$) increase in the drug EE% when the amount of tween 80 was increased. However, a notable decrease of the EE% was observed with further increases of tween 80 amounts (F12<F11<F5). The vesicular bilayer is softened by the addition of tween80, which increases the flexibility of the bilayer and thereby enhances the drug's permeation into vesicles. The incorporation of tween 80, a nonionic surfactant, enhances the flexibility of the vesicular bilayer, thereby facilitating improved drug incorporation into the vesicles. Nonetheless, at higher concentrations, tween 80 increases membrane fluidity to an extent that promotes drug leakage into the surrounding aqueous phase. This is likely due to its hydrophilic nature, which can compromise bilayer integrity and reduce overall entrapment efficiency [23].

Using SDC as edge activator revealed higher EE % compared to tween 80 (table 2). The observed variation may be attributed to the differing interactions between span 60 and the selected edge activators. Span 60, a nonionic surfactant with a high phase transition temperature, forms rigid and stable bilayers that are less permeable to drug leakage [9]. The incorporation of SDC, an anionic surfactant (HLB=16.7), enhances membrane flexibility without compromising vesicle stability, thereby facilitating greater drug encapsulation. In contrast, tween 80 (HLB=15), with its large hydrophilic head group, may disrupt the structural integrity of the span 60 bilayer. These findings are consistent with previous studies indicating the superior performance of SDC in enhancing drug loading within vesicular systems [24, 25].

The effects of increasing SDC amount caused statistically significant ($p<0.01$) decreasing in the EE% when its quantity was increased, as shown in fig. 2B. This is because the likelihood of the formation of mixed micelles with increase the amount of SDC. Furthermore, the fluidity and permeability of the vesicular membranes is enhanced by elevated SDC levels, which results in a decrease in the EE% of FLC. The results agreed with Hadi H and Hussein a who studied the effect of SDC concentration, as an edge activator, for preparation of stable ondansetronHCl-loaded tansfersomal dispersion [26]. On another study, Salem H F *et al.* concluded that SDC, example of bile salt, can integrate into bilayer membranes, imparting enhanced elasticity and surface charge, which stabilizes vesicles and improves EE% by reducing leakage [27].

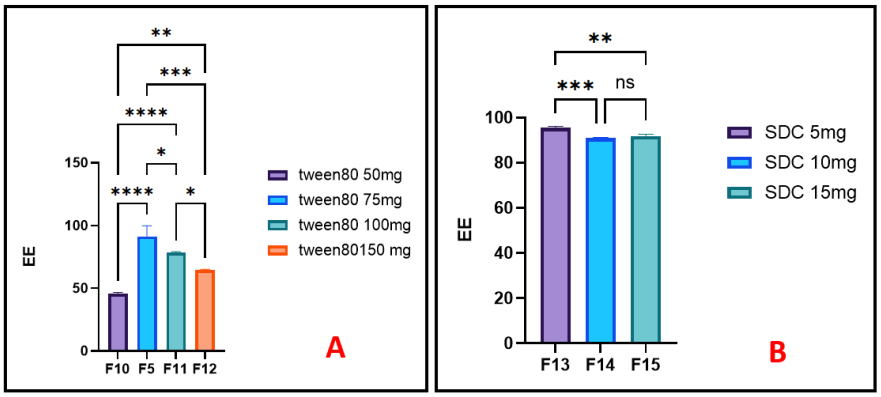

Fig. 2:The effect of different amount of (A) Tween 80 and (B) SDC, edge activators,onentrapmentefficiency of FLC-loaded spanethosomes, (ns,*, ** and * represent non-significant, P<0.05, P<0.01 and P<0.001 respectively), n=3, mean values±SD**

Characterization of spanethosomes vesicular size and PDI

The statistical analysis of the effect of increasing ethanol volume on the size of spanethosomes, while maintaining a constant span 60 amount as illustrated in fig. 3A-C, revealed a significant increase in vesicle size ($P<0.01$), particularly when 4 ml of ethanol used in formulas F3, F6, F9, they showed dramatic incease in size about 3517 as shown in fig. 4, 1803 and 745 nm, respectively. The unusually large vesicle size may due to the excessive ethanol content (4 ml), which likely disrupted optimal vesicle formation by altering lipid packing or destabilizing the bilayer structure. This disruption could lead to vesicle aggregation or fusion, ultimately increasing particle size. Similar observations were reported by Sallustio *et al.* [28], who found that increasing ethanol concentration up to a certain threshold can reduce vesicle size by enhancing membrane fluidity. However, beyond that limit, ethanol may cause bilayer expansion and reduced vesicle stability, contributing to increased vesicle size.

Moreover, it was evident that increasing the amount of span 60 also led to an increase in vesicle size. In comparison with previous studies which reported a decrease in vesicle size with higher ethanol concentrations, have attributed to ethanol-induced bilayer fluidization and interpenetration into lipid chains by hydrogen-bond interaction with polar head of lipid. Further addition may lead to bilayer destabilization or vesicle aggregation, resulting in larger vesicles [29, 30]. Additionally, an increase in span 60: tween 80 ratios from 1.3:1 to 2.6:1 and 4:1 led to a proportional decrease in vesicle size that hinder the flexibility of the bilayer membranes of spanethosomes and, thus, decrease the elasticity of the vesicles and water uptake so leading to decrease in the nanovesicles' size [31].

The mean vesicle size also showed a significant decrease ($P<0.05$) with increasing amounts of Tween 80 as illustrated in fig. 5A for formulas F10>F5>F11>F12. These findings are consistent with those of Almuqbil R *et al.* [32] and Abdelbari M *et al.* [33], who reported that tween 80 acts as an intercalating agent with unsaturated alkyl chain. It reduces surface energy and enhances membrane bilayer bending, thereby decreasing vesicle size and preventing vesicle aggregation. On the other hand, the vesicle size also showed a statistically significant decrease ($P<0.05$) with increasing amounts of SDC, as shown in fig. 5B; F13>F14. Similar findings were reported by Leonyza A [34]. The reduction in vesicle size was attributed to increased membrane curvature and electrostatic repulsion between charged molecules on the outer membrane surface, which reduced vesicle aggregation and inhibited crystal growth. Additionally, the small particle size may be influenced by the high hydrophilic-lipophilic balance (HLB) value of SDC [35].

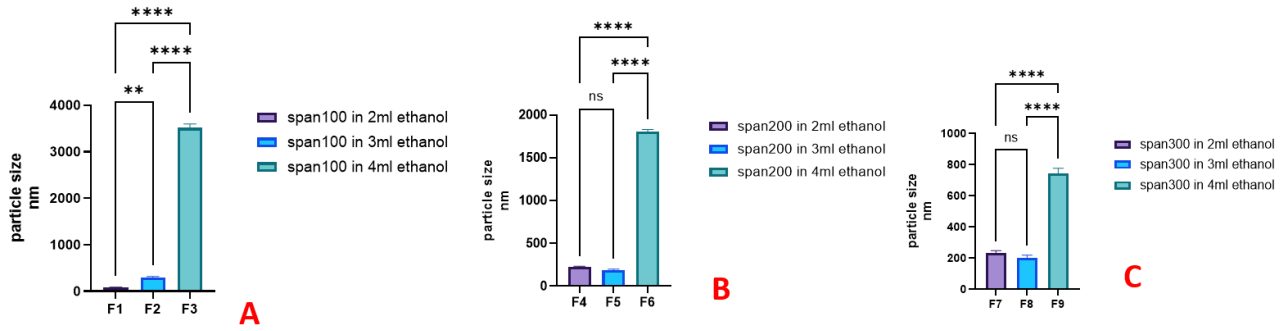

Fig. 3: The impactof ethanol volume on FLC-loaded spanethosomes vesicles size at three level of span 60;(A) 100 mg, (B) 200 mg and (C) 300 mg, (ns,*, ** and * represent non-significant, P<0.05, P<0.01 and P<0.001, respectively), n=3, mean values±SD**

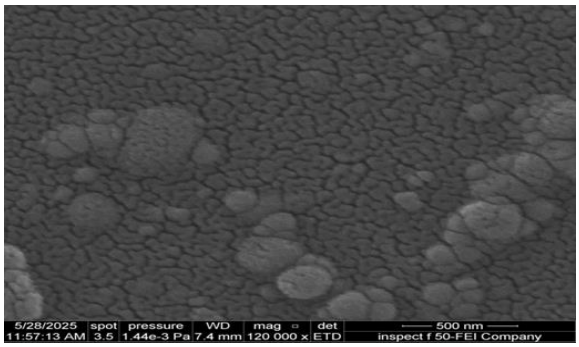

Fig. 4: The surface morphological photo of FLC spanethosme dispersion by SEM (120Kx magnification) (formula F3)

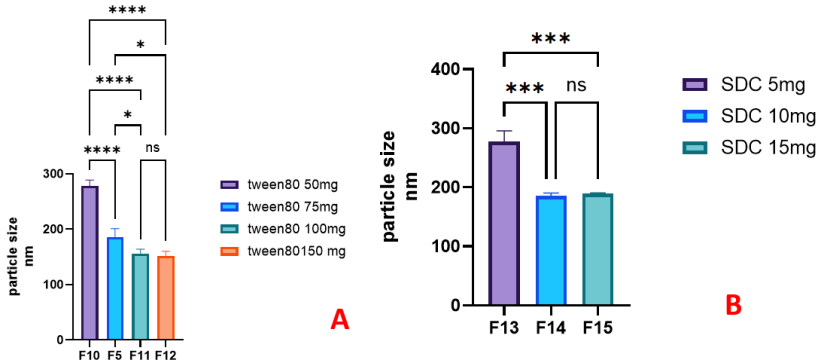

Fig. 5: The impact of edge activatorsamounton FLC-loaded spanethosomes vesicles size, (A) tween 80and (B) sodium deoxycholate (SDC), (ns,*, ** and * represent non-significant, P<0.05, P<0.01 and P<0.001, respectively), n=3, mean values±SD**

The PDI of all prepared formulations was between 0.06±0.02 and 0.51±0.01 (table 2). According to an ANOVA test, the variables including span60 amount, ethanol volume and edge activator amount had a significant (P<0.05) influence on the values of PDI for FLC-loaded spanethosomes. Generally, a PDI value below 0.3 indicates a homogeneous dispersion, reflectinga narrow particle size distribution in the colloidal systems [36]. The formulations F1, F2, F5, F6, F8, F11, F12 and F15 exhibited approximately monodisperse system.

A high PDI (such as in F4, PDI = 0.51) suggested the heterogeneous size distribution, reflecting the coexistence of both small and large vesicle populations within the system. This heterogeneity can negatively impact the physical stability of the system. Smaller vesicles, due to their high surface energy, are more prone to aggregation or fusion, while larger vesicles may be more likely to sediment under gravity over time, both of which can lead to phase separation or drug leakage during storage [37]. Furthermore, a wide size distribution may result in inconsistent vesicle behavior during application. For transdermal delivery, it has been shown that formulations with narrow size distribution (i. e., low PDI) enable more uniform penetration across the stratum corneum, whereas higher PDI may lead to uneven distribution of vesicle sizes on the skin surface. This could reduce the reproducibility and predictability of drug delivery, as different-sized vesicles may follow different penetration pathways or deposit differently within skin layers [38, 39].

In vitro drug release of the selected spanethosomes formulations

Based on the criteria of EE% greater than 90%, vesicles size less than 300 nm and PDI below 0.3 for the collected data (table 2), the formulations F2, F5 and F15 were selected for comparison their dissolution profiles.

As observed in fig. 6, the percentage of FLC released from the spanethosomes formulations after 6 h followed the order: F5 (100±0.0%)>F2 (95.15±1.32%)>F15 (94.60±1.64%). A comparison of their dissolution profiles revealed that all three formulations exhibited a similarity factor (*f2*) of less than 50 (table 3), indicating a significant difference in their dissolution behavior [40]. Notably, the majority of the release (around 50%) occurred within the first 2 h. This rapid initial release can be attributed to the smaller particle size of formulations F2 and F5, as its reduced vesicle diameter likely

facilitated quicker diffusion of the drug into the aqueous dissolution medium [41]. On the contrary, the formulation F15 containing SDC exhibited a slower initial release of FLC, ultimately reaching 94.6% after 6 h. This agree with El Zaafarany G [24] and Ali S [42], who attributed the slower initial drug release with SDC is due to its rigid integration into the vesicle membrane, enhancing stability and reducing permeability, unlike tween 80, which fluidizes the bilayer and promotes faster release.

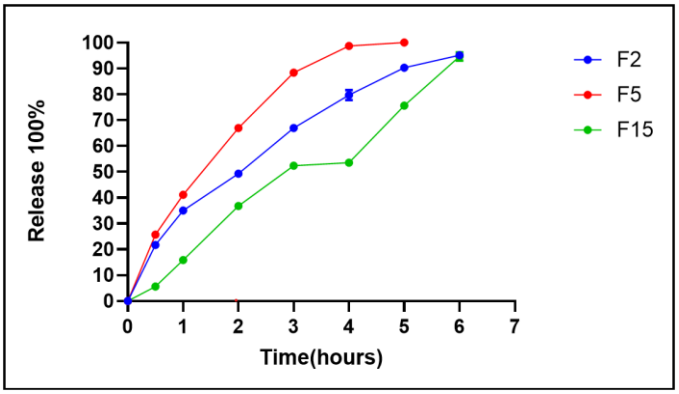

Fig. 6: The dissolution profile of the selected FLC-loaded spanethosomes formulations

Table 3: Similarity factor *f2* for comparison of dissolution profiles of the selected FLC spanethosomes dispersion

Formula code	F2	F5	F15
f2 compare to F2 (standard)	---	43.814	40.584
*f2*compare to F5 (standard)	43.814	----	27.924
f2 compare to F15 (standard)	40.584	27.924	----

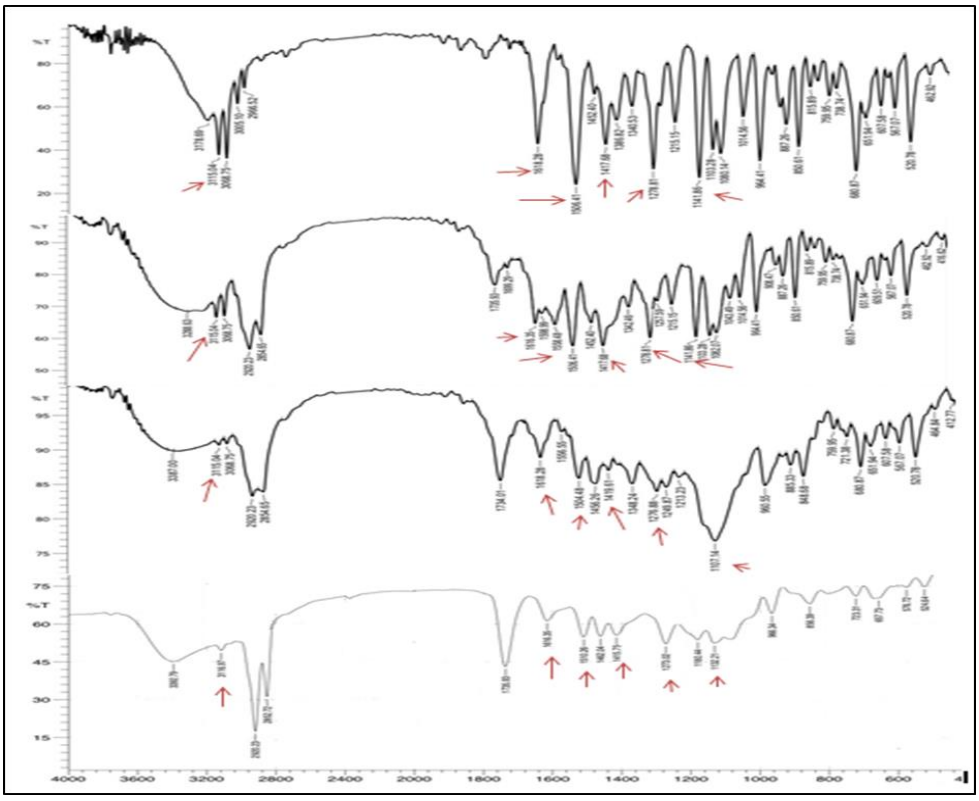

Fig. 7: The FTIR spactra of FLC, physical mixture of FLC: span 60: tween 80, physical mixture of FLC: span 60: SDC and formula F15 for up to down, respectively

Optimization of FLC spanethosomes

Formula F15 was chosen as the optimum formula for further investigation in light of the results. Since it exhibited an optimal nanosize (188.7.00±1.8 nm), PDI (0.25±0.01). Additionally, it demonstrated an acceptable EE (91.91±0.80%) and FLC release rate of approximately 94.6% at 6 h.

Fourier-transform infrared spectra (FT-IR)

The FTIR spectra of pure FLC, physical mixture and the optimum formula (F15) were shown in fig. 7. The FTIR spectrum of FLC displayed key characteristic bands at approximately 3115.04 cm^{-1} (O–H and aromatic C–H stretching), 1618.28 cm^{-1} (aromatic C=C stretching), 1506.41 and 1417.68 cm^{-1} (triazole ring stretching),

1278.81 cm^{-1} (C–F stretching), 1141.86 cm^{-1} (C–O tertiary alcohol stretching), and 964 cm^{-1} (C–H bending vibrations). These findings align with previously reported spectra and confirm the presence of FLC functional groups [43, 44]. The FTIR spectra of the physical mixture showed all characteristic peaks of FLC as well as the used excipients without the appearance of new bands, indicating the absence of chemical interaction. Slight boarding in the O–H and C=O regions suggest possible hydrogen bonding or physical associations among the components. The spectrum of the formula F15 exhibited all major characteristicpeaks of FLC as illustrated in fig. 7 confirms the chemical integrity of FLC [45]. Notably, there were reduction in peaks intensity with minor deviation of peak at 1141.86 cm^{-1} to 1132.21 cm^{-1} which may indicate partial amorphization or dispersion at the molecular level, which is expected in vesicular systems [46].

The characteristic X-ray diffraction (XRD) patterns of FLC were compared with those of its physical mixture and the final formulation (F15), as illustrated in fig. 8. The diffraction pattern of pure FLC showed sharp peaks at 2θ angles of 14.93°, 17.39°, 19.5°, 24.55°, 26.91°, and 29.31°, indicating its crystalline nature. These findings are in agreement with the previous report by Modha *et al.* [47]. The diffractogram of the physical mixture exhibited all the characteristic peaks of FLC, albeit with reduced intensity, indicating no significant change in the drug's crystallinity. Additionally, a new peak appeared in the physical mixture, which may be attributed to Span 60, as reported by Yassin GE *et al.* [48]. Meanwhile, the diffractogram of formulation F15 demonstrated the complete absence of the sharp crystalline peaks of FLC except for a broad peak around 21° (2θ). This confirms the transformation of FLC from its crystalline form to an amorphous state, likely encapsulated within the vesicular system. These results are consistent with previous findings [49].

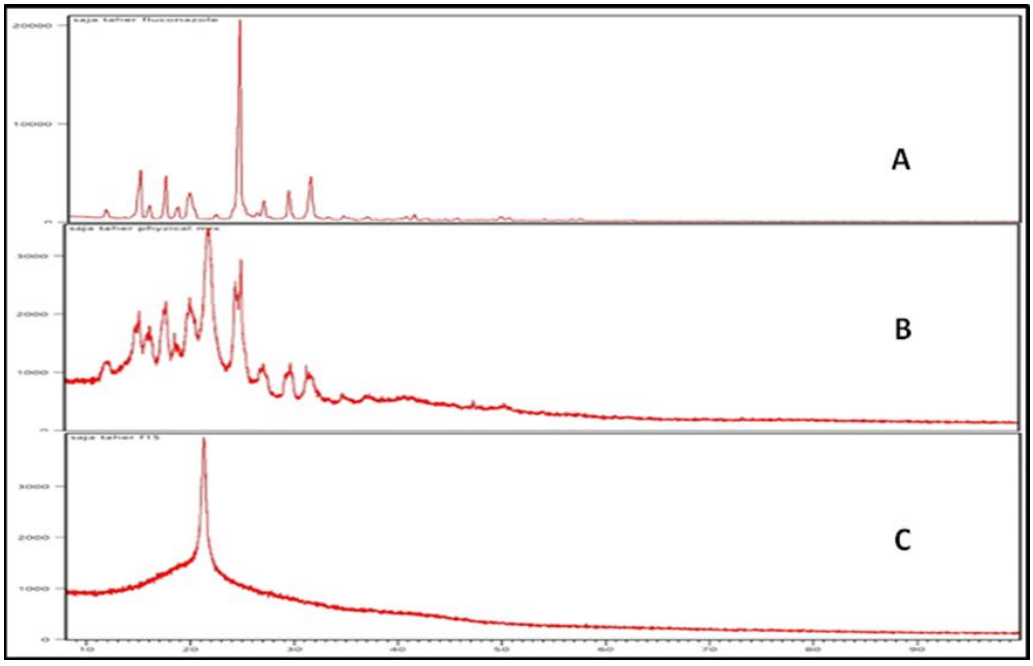

Fig. 8: The X-ray spactra of (A) FLC, (B) physical mixture of fluconazole: span 60: SDC and (C) formula F15

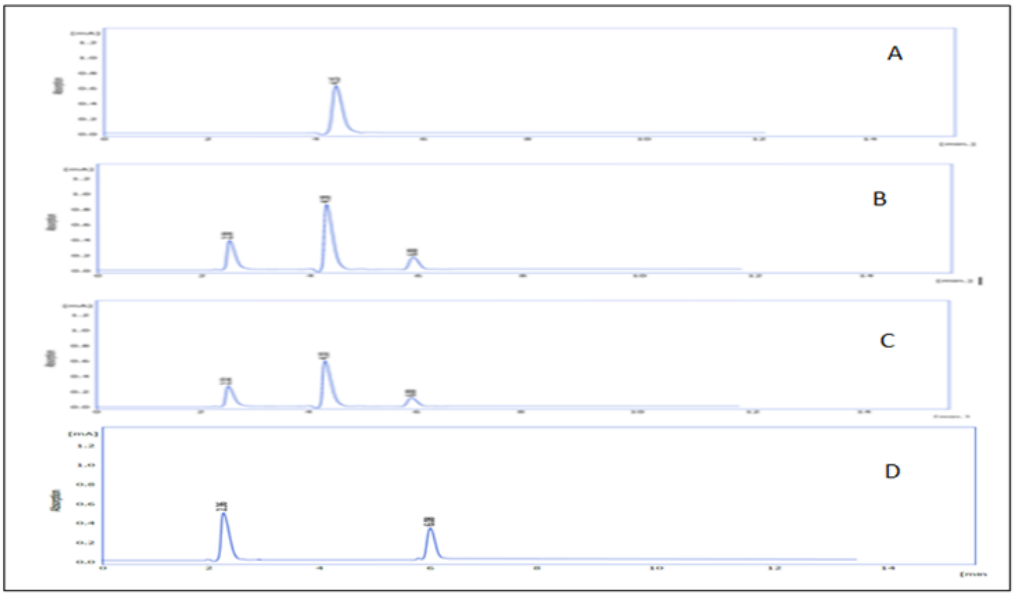

Fig. 9: The HPLC chromatograms: (A) Pure FLC, (B) Fresh F15 formulation, (C) F15 after 3 mo of storage at room temperature, (D) Blank F15

Assessment of FLC stability in spanethosomeformulations

The analysis HPLC showed consistent retention times (RT) for FLC across samples: 4.15 min for pure drug, 4.18 min for freshly prepared F15, and 4.10 min for F15 stored at room temperature for 3 mo (fig. 9 A-C). This minor variation indicates that FLC remained chemically stable, with no signs of degradation or new peak formation. Two additional peaks (approximately 2.3 and 6.0 min) were observed in both the F15 and blank formulations (fig. 9D), attributed to formulation excipients, not degradation products. These findings are supported by recent validated HPLC studies that confirm fluconazole's stability under various storage conditions and analytical methods [50]. Additionally, modern vesicular system like novasomes, has demonstrated protective effects on FLC stability during storage [44]. Thus, the F15 formulation effectively preserves FLC's chemical integrity over time.

Surface morphology determination

Microscopy photo (fig. 10, left) confirmed the presence of spherical vesicles with a well-defined outer boundary. The dispersion appeared uniform, with no signs of aggregation. Additionally, the SEM imaging (fig. 10, right) supported these findings, revealing smooth, discrete vesicles with intact morphology. These observations are in agreement with previous studies, which similarly demonstrated stable, well-formed fluconazole-loaded transfersomal vesicles using electron microscopy [51].

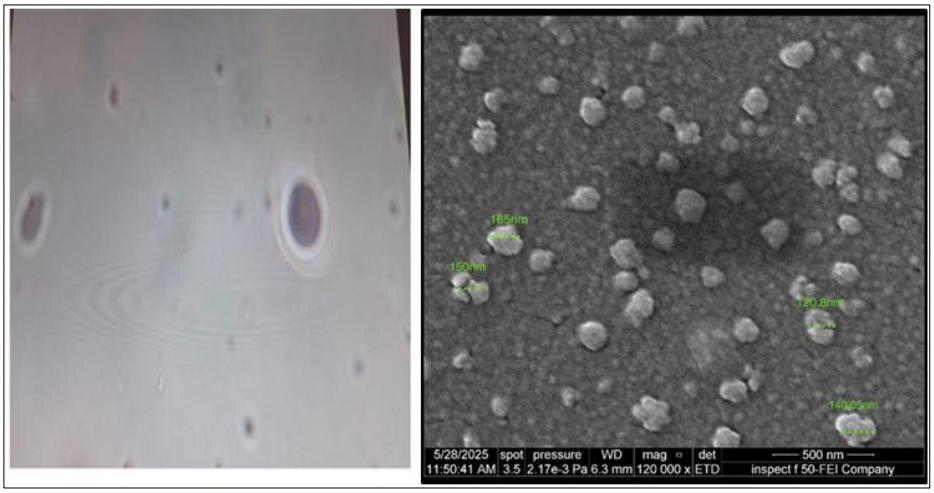

Fig. 10: Surface morphological photos of FLC spanethosomes taken by; (left) optical microscope, and (right) SEM (120Kx magnification, 500 nm scale)

CONCULSION

The ethanol injection method was employed to effectively prepare FLC spanethosome in the present study. A promising drug carrier was introduced in the form of FLC spanethosome dispersion, which can be applied topically or incorporated into a topical dosage form. FLCspanethosome entrapment efficiency and vesicle size decreased as more amount of sodium deoxycholate introduced. The optimized FLC formula (F15) exhibited a nanosized range, high entrapment efficiency, and 94.6% of drug release over 6 h. The dispersion will be later incorporated into a gel base as the final dosage form. Future work will include stability testing and ex vivo skin permeation studies for gel to confirm formulation robustness and targeting potential.

ACKNOWLEDGEMENT

The authors would like to express their gratitude to the Department of Pharmaceutics/College of Pharmacy/University of Baghdad for their assistance and support in conducting this study in their laboratories.

FUNDING

There is no financial assistance available.

AUTHORS CONTRIBUTIONS

The authors confirm contribution to the paper as follows: study conception and design: LubnaA. Sabri (L. A. S.); data collection: Saja Taher (S. T.); analysis and interpretation of results: L. A. S, S. T.; draft manuscript preparation: L. A. S, S. T. Both authors reviewed the results and approved the final version of the manuscript.

CONFLICTS OF INTERESTS

We affirm that there are no conflicts of interest.

REFRENCES

1. Mosallam S, Albash R, Abdelbari MA. Advanced vesicular systems for antifungal drug delivery. AAPS PharmSciTech. 2022;23(6):206. doi: 10.1208/s12249-022-02357-y, PMID 35896903.
2. Tarannum N, Pooja K, Jakhar S, Mavi A. Nanoparticles assisted intra and transdermic delivery of antifungal ointment: an updated review. Discov Nano. 2024;19(1):11. doi: 10.1186/s11671-023-03932-3, PMID 38195832.
3. Mali R, Patil J. Nanoparticles: a novel antifungal drug delivery system. Mater Proceeding. 2023:14(1):61. doi: 10.3390/IOCN2023-14513.
4. El Housiny S, Shams Eldeen MA, El Attar YA, Salem HA, Attia D, Bendas ER. Fluconazole-loaded solid lipid nanoparticles topical gel for treatment of pityriasis versicolor: formulation and clinical study. Drug Deliv. 2018;25(1):78-90. doi: 10.1080/10717544.2017.1413444, PMID 29239242.
5. Salerno C, Carlucci AM, Bregni C. Study of *in vitro* drug release and percutaneous absorption of fluconazole from topical dosage forms. AAPS PharmSciTech. 2010;11(2):986-93. doi: 10.1208/s12249-010-9457-1, PMID 20521179.
6. Touitou E, Natsheh H. The evolution of emerging nanovesicle technologies for enhanced delivery of molecules into and across the skin. Pharmaceutics. 2024;16(2):267. doi: 10.3390/pharmaceutics16020267, PMID 38399321.
7. El Zaafarany GM, Nasr M. Insightful exploring of advanced nanocarriers for the topical/transdermal treatment of skin diseases. Pharm Dev Technol. 2021;26(10):1136-57. doi: 10.1080/10837450.2021.2004606, PMID 34751091.
8. Sinico C, Fadda AM. Vesicular carriers for dermal drug delivery. Expert Opin Drug Deliv. 2009;6(8):813-25. doi: 10.1517/17425240903071029, PMID 19569979.
9. Alhammid SN, Kassab HJ, Hussein LS, Haiss MA, Alkufi HK. Spanlastics nanovesicles: an emerging and innovative approach for drug delivery. Maaen J Med Sci. 2023;2(3):9-17. doi: 10.55810/2789-9128.1027.
10. Abd Alaziz DM, Mansour M, Nasr M, Sammour OA. Spanethosomes as a novel topical carrier for silymarin in contrast to conventional spanlastics: formulation development

in vitro and ex vivo evaluation for potential treatment of leishmaniasis. J Drug Deliv Sci Technol. 2023 Aug;88:104887. doi: 10.1016/j.jddst.2023.104887.
11. Richard C, Cassel S, Blanzat M. Vesicular systems for dermal and transdermal drug delivery. RSC Adv. 2020;11(1):442-51. doi: 10.1039/D0RA09561C, PMID 35423006.
12. Al Sawaf OF, Al gawhari FJ. Novel probe sonication method for the preparation of meloxicam bilosomes for transdermal delivery: part one. J Res Med Dent Sci. 2023;11(6):5-12.
13. Al Edhari GH, Al Gawhari FJ. Study the effect of formulation variables on preparation of nisoldipine loaded nano bilosomes. IJPS. 2023;32Suppl:271-82. doi: 10.31351/vol32issSuppl.pp271-282.
14. Almajidi YQ, Taghi H, Issa AA. Formulation and development of ethosomal drug delivery system of silymarin for transdermal application. Iraqi J Pharm Sci. 2024;33(4):126-40. doi: 10.31351/vol33iss4pp126-140.
15. Abdelmalak NS, El Menshawe SF. A new topical fluconazole microsponge loaded hydrogel: preparation and characterization. Int J Pharm Pharm Sci. 2012;4Suppl1:460-9.
16. Rajab NA, Talal Sulaiman H. Olmesartan medoxomil nanomicelle using soluplus for dissolution enhancement preparation *in vitro* and ex-vivo evaluation. Iraqi J Pharm Sci. 2025 Jun;34(2):47-59. doi: 10.31351/vol34iss2pp47-59.
17. Jassim ZE, Al Kinani KK, Alwan ZS. Preparation and evaluation of pharmaceutical cocrystals for solubility enhancement of dextromethorphan HBr. Int J Drug Deliv Technol. 2021 Oct 1;11(4):1342-9. doi: 10.25258/ijddt.11.4.37.
18. Liew KB, Loh GO, Tan YT, Peh KK. Development and application of simple HPLC-UV method for fluconazole quantification in human plasma. Int J Pharm Pharm Sci. 2012;4(4):107-1011.
19. Alkufi HK, Kassab H. A potential method for enhanced performance of nimodipine by Spanlastic nanovesicle with tween 40 as edge activator. Iraqi J Pharm Sci. 2025 Jun;34(2):227-38. doi: 10.31351/vol34iss2pp227-238.
20. Bhalaria MK, Naik S, Misra AN. Ethosomes: a novel delivery system for antifungal drugs in the treatment of topical fungal diseases. Indian J Exp Biol. 2009;47(5):368-75. PMID 19579803.
21. Kumar GP, Rajeshwarrao P. Nonionic surfactant vesicular systems for effective drug delivery an overview. Acta Pharmacol Sin B. 2011;1(4):208-19. doi: 10.1016/j.apsb.2011.09.002.
22. Shaji J, Shah A. Optimisation of tenoxicam-loaded niosomes using quadratic design. Int J Curr Pharm Sci. 2016 Jan 7;8(1):62-7.
23. Elsayed MM, Ibrahim MM, Cevc G. The effect of membrane softeners on rigidity of lipid vesicle bilayers: derivation from vesicle size changes. Chem Phys Lipids. 2018 Jan;210:98-108. doi: 10.1016/j.chemphyslip.2017.10.008, PMID 29107604.
24. El Zaafarany GM, Awad GA, Holayel SM, Mortada ND. Role of edge activators and surface charge in developing ultradeformable vesicles with enhanced skin delivery. Int J Pharm. 2010 Sep 15;397(1-2):164-72. doi: 10.1016/j.ijpharm.2010.06.034, PMID 20599487.
25. Shaji J, Lal M. Preparation optimization and evaluation of transferosomal formulation for enhanced transdermal delivery of a COX-2 inhibitor. Int J Pharm Pharm Sci. 2014;6(1):467-77.
26. Hadi HA, Hussein AH. Effect of addition a sodium deoxycholate as an edge activator for preparation of ondansetron HCL tansfersomal dispersion. AJPS. 2023;23(4):429-42. doi: 10.32947/ajps.v23i4.1097.
27. Salem HF, Nafady MM, Ali AA, Khalil NM, Elsisi AA. Evaluation of metformin hydrochloride-tailored bilosomes as an effective transdermal nanocarrier. Int J Nanomedicine. 2022 Mar 17;17:1185-201. doi: 10.2147/IJN.S345505, PMID 35330695.
28. Sallustio V, Farruggia G, Di Cagno MP, Tzanova MM, Marto J, Ribeiro H. Design and characterization of an ethosomal gel encapsulating rosehip extract. Gels. 2023 Apr 25;9(5):362. doi: 10.3390/gels9050362, PMID 37232954.
29. Limsuwan T, Boonme P, Khongkow P, Amnuaikit T. Ethosomes of phenylethyl resorcinol as vesicular delivery system for skin lightening applications. BioMed Res Int. 2017;2017:8310979. doi: 10.1155/2017/8310979, PMID 28804723.
30. Patra M, Salonen E, Terama E, Vattulainen I, Faller R, Lee BW. Under the influence of alcohol: the effect of ethanol and methanol on lipid bilayers. Biophys J. 2006 Feb 15;90(4):1121-35. doi: 10.1529/biophysj.105.062364, PMID 16326895.
31. Said M, Ali KM, Alfadhel MM, Afzal O, Aldosari BN, Alsunbul M. Ocular mucoadhesive and biodegradable spanlastics loaded cationic spongy insert for enhancing and sustaining the anti-inflammatory effect of prednisolone na phosphate; preparation i-optimal optimization and *in vivo* evaluation. Int J Pharm X. 2024 Oct 16;8:100293. doi: 10.1016/j.ijpx.2024.100293, PMID 39498272.
32. Almuqbil RM, Sreeharsha N, Nair AB. Formulation by design of efinaconazole spanlastic nanovesicles for transungual delivery using statistical risk management and multivariate analytical techniques. Pharmaceutics. 2022 Jul 6;14(7):1419. doi: 10.3390/pharmaceutics14071419, PMID 35890316.
33. Abdelbari MA, El Mancy SS, Elshafeey AH, Abdelbary AA. Implementing spanlastics for improving the ocular delivery of clotrimazole: *in vitro* characterization ex vivo permeability microbiological assessment and *in vivo* safety study. Int J Nanomedicine. 2021;16:6249-61. doi: 10.2147/IJN.S319348, PMID 34531656.
34. Leonyza A, Surini S. Optimaztion of sodium deoxycholate-based transferosomes for percutaneous delivery of peptides and proteins. Int J Appl Pharm. 2019;11(5):329-32. doi: 10.22159/ijap.2019v11i5.33615.
35. Hassan AS, Hofni A, Abourehab MA, Abdel Rahman IA. Ginger extract-loaded transethosomes for effective transdermal permeation and anti-inflammation in rat model. Int J Nanomedicine. 2023;18:1259-80. doi: 10.2147/IJN.S400604, PMID 36945254.
36. Danaei M, Dehghankhold M, Ataei S, Hasanzadeh Davarani F, Javanmard R, Dokhani A. Impact of particle size and polydispersity index on the clinical applications of lipidic nanocarrier systems. Pharmaceutics. 2018 May 18;10(2):57. doi: 10.3390/pharmaceutics10020057, PMID 29783687.
37. Guillot AJ, Martinez Navarrete M, Garrigues TM, Melero A. Skin drug delivery using lipid vesicles: a starting guideline for their development. J Control Release. 2023 Mar;355:624-54. doi: 10.1016/j.jconrel.2023.02.006, PMID 36775245.
38. Guo F, Wang J, Ma M, Tan F, Li N. Skin-targeted lipid vesicles as novel nano-carrier of ketoconazole: characterization *in vitro* and *in vivo* evaluation. J Mater Sci Mater Med. 2015 Apr;26(4):175. doi: 10.1007/s10856-015-5487-2, PMID 25825320.
39. Deaguero IG, Huda MN, Rodriguez V, Zicari J, Al Hilal TA, Badruddoza AZ. Nano-vesicle-based anti-fungal formulation shows higher stability skin diffusion, biosafety and anti-fungal efficacy *in vitro*. Pharmaceutics. 2020 Jun 5;12(6):516. doi: 10.3390/pharmaceutics12060516, PMID 32517047.
40. Kadhum RW, Abd Alhammid SN. Preparation and characterization of dutasteride nanoparticles as oral fast-dissolving film. J Fac Med Baghdad. 2024 Jul;66(2):237-46. doi: 10.32007/jfacmedbagdad.6622240.
41. Elgewelly MA, Elmasry SM, Sayed NS, Abbas H. Resveratrol loaded vesicular elastic nanocarriers gel in imiquimod-induced psoriasis treatment: *in vitro* and in vivo evaluation. J Pharm Sci. 2022 Feb;111(2):417-31. doi: 10.1016/j.xphs.2021.08.023, PMID 34461114.
42. Ali SK, Entidhar J, Al Akkam. Bilosomes as soft nanovesicular carriers for ropinirole hydrochloride: preparation and *in vitro* characterization. IJPS. 2023;32Suppl:177-87. doi: 10.31351/vol32issSuppl.pp177-187.
43. Rathi R, Singh I, Sangnim T, Huanbutta K. Development and evaluation of fluconazole co-crystal for improved solubility and mechanical properties. Pharmaceutics. 2025;17(3):371. doi: 10.3390/pharmaceutics17030371, PMID 40143034.
44. Fatima I, Rasul A, Shah S, Saadullah M, Islam N, Khames A. Novasomes as nano-vesicular carriers to enhance topical delivery of fluconazole: a new approach to treat fungal infections. Molecules. 2022;27(9):2936. doi: 10.3390/molecules27092936, PMID 35566287.
45. Rajeshwar V, Kondoju DL, Bushra F, Vasudha B. Development and evaluation of liposomal selexipag: a novel oral delivery system for pulmonary arterial hypertension. Asian J Pharm Clin Res. 2025 Jul 7;18(7):167-73. doi: 10.22159/ajpcr.2025v18i7.54840.
46. Adhikari S, Sudheer P, Mohana B, Manjunatha PS. Design development and evaluation of doxorubicin hydrochloride-loaded transfersomes for transdermal drug delivery. Thai J Pharm Sci. 2024;48(2):1-11. doi: 10.56808/3027-7922.2907.

47. Modha NB, Chotai NP, Patel VA, Patel BG. Preparation characterization and evaluation of fluconazole polymorphs. Int J Res Pharm Biomed Sci. 2010;1(2):124-7.
48. Yassin GE, Amer MA, Mannaa IM, Khalifa MK. Fluconazole noisome-laden contact lens: a promising therapeutic approach for prolonged ocular delivery and enhanced antifungal activity. J Pharm Innov. 2024 Aug;19(4):45. doi: 10.1007/s12247-024-09850-w.
49. Zaki RM, Alfadhel MM, Alossaimi MA, Elsawaf LA, Devanathadesikan Seshadri V, Almurshedi AS. Central composite optimization of Glycerosomes for the enhanced oral bioavailability and brain delivery of quetiapine fumarate. Pharmaceuticals (Basel). 2022;15(8):940. doi: 10.3390/ph15080940, PMID 36015089.
50. Macartney RA, Fricker AT, Smith AM, Fedele S, Roy I, Knowles JC. A RP-HPLC-UV method for the dual detection of fluconazole and clobetasol propionate and application to a model dual drug delivery hydrogel. Anal Methods. 2025;17(18):3694-704. doi: 10.1039/D4AY02219J, PMID 40269534.
51. Cheng Z, Kandekar U, Ma X, Bhabad V, Pandit A, Liu L. Optimizing fluconazole embedded transfersomal gel for enhanced antifungal activity and compatibility studies. Front Pharmacol. 2024 Mar 28;15:1353791. doi: 10.3389/fphar.2024.1353791, PMID 38606182.